

All-Optical Demultiplexing from 160 to 40/80 Gb/s Using Mach-Zehnder Switches Based on Intersubband Transition of InGaAs/AlAsSb Coupled Double Quantum Wells

Ryoichi AKIMOTO^{†a)}, Guangwei CONG[†], Masanori NAGASE[†], Teruo MOZUME[†], *Nonmembers*, Hidemi TSUCHIDA^{††}, Toshifumi HASAMA[†], and Hiroshi ISHIKAWA[†], *Members*

SUMMARY We demonstrated all-optical demultiplexing of 160-Gb/s signal to 40- and 80-Gb/s by a Mach-Zehnder Interferometric all-optical switch, where the picosecond cross-phase modulation (XPM) induced by intersubband excitation in InGaAs/AlAsSb coupled double quantum wells is utilized. A bi-directional pump configuration, i.e., two control pulses are injected from both sides of a waveguide chip simultaneously, increases a nonlinear phase shift twice in comparison with injection of single pump beam with forward- and backward direction. The bi-directional pump configuration is the effective way to avoid damaging waveguide facets in the case where high optical power of control pulse is necessary to be injected for optical gating at repetition rate of 40/80 GHz. Bit error rate (BER) measurements on 40-Gb/s demultiplexed signal show that the power penalty is decreased slightly for the bi-directional pump case in the BER range less than $\sim 10^{-6}$. The power penalty is 1.3 dB at BER of 10^{-9} for the bi-directional pump case, while it increases by 0.3–0.6 dB for single pump cases. A power penalty is influenced mainly by signal attenuation at “off” state due to the insufficient nonlinear phase shift, upper limit of which is constrained by the current low XPM efficiency of ~ 0.1 rad/pJ and the damage threshold power of ~ 100 mW in a waveguide facet.

key words: intersubband transition, coupled double quantum well, cross-phase modulation, Mach-Zehnder interferometer, all-optical demultiplexing

1. Introduction

All optical demultiplexing is one of the key functions for optical signal processing in high-bit-rate (above 160 Gbit/s) optical time division multiplexing (OTDM) system. Currently, demultiplexers based on fiber [1], [2] and semiconductor optical amplifier [3]–[5] have been investigated intensively at data-rates of 160-Gb/s and beyond. The latter is semiconductor-based and has advantages such as miniaturization of the system, high stability and low switching power, however, a pattern effect due to a slow carrier relaxation, inherent in an interband transition, is regarded as a potential issue at a high-speed operation. Intersubband transitions (ISBT) in semiconductors quantum wells (QWs) is another candidate for a semiconductor-based demultiplexer,

since a typical ISBT carrier relaxation time in a QW is of the order of sub- to a few picoseconds (ps), expecting it is free from the pattern effect. Several groups have reported on ISBT waveguide switches with a switching response of a few ps to sub-ps at the optical communication wavelength of $\lambda = 1.55 \mu\text{m}$ in material systems, such as InGaAs/AlAs/AlAsSb QWs [6], [7], GaN/AlN QWs [8], [9], and (CdS/ZnSe)/BeTe QWs [10], [11]. In these devices, the switching principle is based on transverse magnetic (TM) light intensity modulation due to the intersubband absorption saturation and its ultrafast recovery. One major issue in this type of devices is a large insertion loss due to a remaining ISBT absorption during the switch-on state. In general, a large on/off extinction ratio requires a corresponding large absorption at the switch-off state. Thus a switching operation at low energy seems to be incompatible with a low insertion loss at the switch-on state, which would significantly deteriorate the device figure-of-merit in this type of devices.

In ISBT switch utilizing InGaAs/AlAs/AlAsSb QWs, a novel modulation mechanism was reported, in which transverse electric (TE) light immune to the absorption is phase-modulated by ISBT excitation by TM light [12]. This is interesting modulation mechanism, since TE light does not suffer from a large insertion loss due to the strong intersubband absorption. Thus we could realize a device with low insertion loss at switch-on state by using this novel mechanism. As for the origin of the cross-phase modulation, two models were suggested, i.e., carrier-plasma dispersion model and interband dispersion model [13]. Although the carrier-plasma dispersion model was concluded as a dominant contribution to the cross phase modulation (XPM) in Ref.13, a recent study revealed that a XPM efficiency is enhanced significantly as the probe wavelength approaches to the interband absorption edge, showing the evidence that the interband dispersion model is a dominant mechanism [14]. An all-optical wavelength conversion at 10 Gb/s [12], a demultiplexing of 160- to 10 Gb/s [15], and a sinusoidal modulation at repetition rate as high as 76 GHz [16] have been reported by utilizing the cross-phase modulation effect.

In this contribution, we report on a demultiplexing of 160-Gb/s signal with the optical gating at higher repetition rates such as 40- and 80 GHz by Mach-Zehnder Interferometer (MZI) ISBT switches. This higher frequency operation is enabled by use of improved quantum well struc-

Manuscript received July 8, 2008.

Manuscript revised October 24, 2008.

[†]The authors are with Network Photonics Research Center, National Institute of Advanced Industrial Science and Technology (AIST), Tsukuba-shi, 305-8568 Japan.

^{††}The author is with Photonics Research Institute, National Institute of Advanced Industrial Science and Technology (AIST), AIST Tsukuba Central 2-1, Tsukuba-shi, 305-8568 Japan.

a) E-mail: r-akimoto@aist.go.jp

DOI: 10.1587/transele.E92.C.187

ture as well as a bi-directional pump configuration. The dependence of pump injection direction on XPM efficiency is discussed. Then the experimental results of demultiplexing from 160 Gb/s to 40- and 80 Gb/s by means of bi-directional pump or single pump configurations are shown. The dependence of the power penalty on these pump configurations is discussed.

2. Bi-directional Pump

Figures 1(a) and (b) show a photo and the schematic of the MZI-ISBT switch module, respectively. The detail of the operation principle of the MZI-ISBT switch was already reported elsewhere [15]. In the present module, a 150 μm -long high-mesa waveguide chip with improved XPM efficiency (about two times higher, compared with a previous waveguide) is installed [17]. The waveguide layer was grown by molecular beam epitaxy on InP substrate that works as a bottom cladding layer. The epitaxial layer structure consists of a 500-nm-thick core layer of a separate confinement heterostructure (a 90 nm-thick bottom optical guiding, a 370 nm-thick active, a 40 nm-thick upper optical guiding layers) and a 1- μm -thick upper InAlAs cladding layer. The active layer is formed by 40 periods of coupled double quantum well (CDQW), where one period of CDQW is composed of $\text{In}_{0.53}\text{Ga}_{0.47}\text{As}(2.7\text{ nm})/\text{In}_{0.52}\text{Al}_{0.48}\text{As}(4\text{ ML})/\text{In}_{0.53}\text{Ga}_{0.47}\text{As}(2.7\text{ nm})/\text{AlAs}(1\text{ ML})/\text{AlAs}_{0.49}\text{Sb}_{0.51}(2\text{ nm})$ and the InGaAs wells are doped with Si of $9 \times 10^{18}/\text{cm}^3$. The bottom and upper optical guiding layers are composed of 10 and 5 periods of CDQW, respectively. The CDQW structure in the optical guiding layers is the same as one in the active layer except that it has no AlAs (1ML) interlayer

and InGaAs wells are left undoped. The optical confinement factor into the active layer is estimated to be 0.55 at $\lambda = 1.55\ \mu\text{m}$, while it reduces to 0.33 after taking into account of a well/barrier thickness ratio.

A bi-directional pump configuration is considered, since this pump configuration can increase an amount of phase shift without damaging a waveguide facet due to high optical power input necessary for gating operation at a repetition rate higher than 40 GHz. A TM pump light (active to ISBT) is split into two and they are launched into the both facets of waveguide as shown in Fig. 1(b). In the present waveguide, we expect there is no substantial difference in XPM efficiency between two propagation directions, since the pump penetration depth ($1/\alpha_{\text{ISBT}} = 31\ \mu\text{m}$) is much smaller than the spatial extension of the pump pulse ($\sim 180\ \mu\text{m}$) in the waveguide. Figure 2 shows the experimental setup for a measurement of nonlinear phase shift, where a TM pump at $\lambda = 1560\ \text{nm}$ excites the intersubband transition between the first and fourth levels formed in CDQWs, and the excitation induces a cross-phase modulation on continuous wave (CW) TE probe at 1541 nm. A mode-locked fiber laser at 10 GHz repetition rate and $\lambda = 1560\ \text{nm}$ is used for a pump. The phase bias of the MZI is adjusted at $\pi/2$. A temporal intensity change of the probe light is monitored by optical sampling scope and the corresponding phase shift is evaluated. Figure 3 shows the phase shift of three MZI-ISBT modules with forward and backward pump configuration as a function of lunched pump pulse energy. The waveguide chips used in these modules are fabricated from the same wafer, and only difference is mesa width. XPM efficiency slope ranges between 0.085–0.112 rad/pJ. No obvious difference in XPM efficiency is observed between the forward and the backward pump configurations. A slight difference in XPM efficiency between two pump configurations could be attributed to fluctuation of coupling efficiency between the waveguide chip and the pump light during manufacturing each module.

We simulate a temporal phase change imposed on the CW TE probe with different TM pump propagation directions, i.e., the forward or the backward propagation with respect to the probe propagation direction. The purpose is

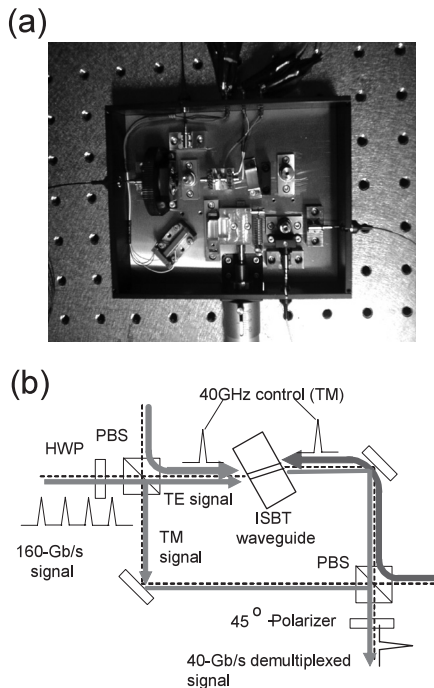


Fig. 1 (a) a photo and (b) schematic of the MZI-ISBT switch module.

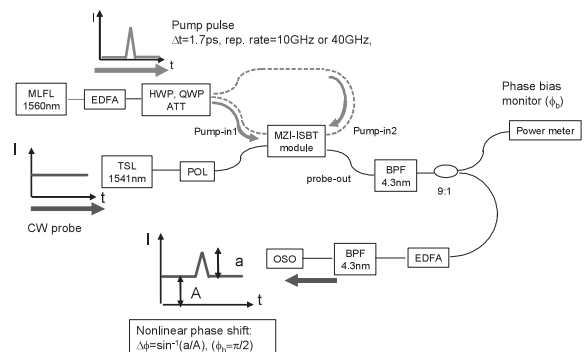


Fig. 2 Schematic of experimental setup for measurement of nonlinear phase shift in forward and backward pump configurations.

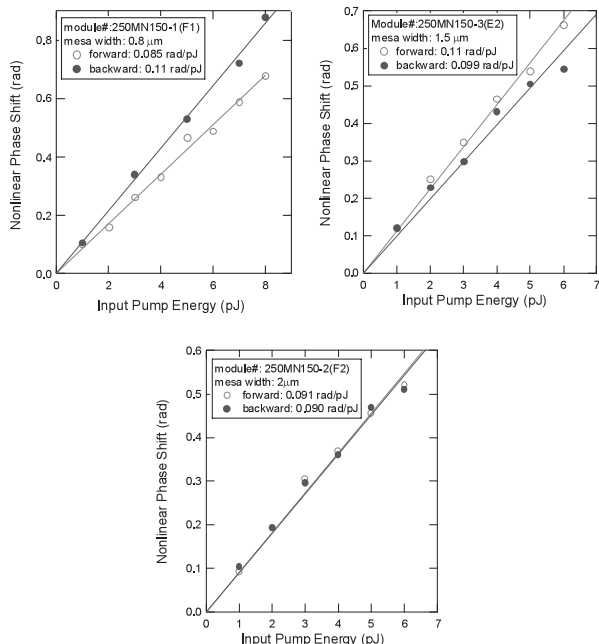


Fig. 3 Nonlinear phase shift as a function of pump pulse energy for three modules which include waveguide chip with different mesa width. For each module, forward and backward pump configurations are compared.

to understand qualitatively the experimental result obtained above, i.e., XPM efficiency does not depend on a pump direction. One-dimensional finite-difference time domain (FDTD) method combined with rate equations describing intersubband carrier dynamics is employed in the simulation. The pump pulse width and the waveguide length are set at 1 ps and 100 μm , respectively. These values are chosen by considering a reasonable balance between the actual experimental situation and the calculation time. In the calculation is divided to two parts, i.e., in the first part a propagation of a pump pulse coupled with an intersubband polarization and carrier rate equations is simulated by the FDTD method, then a carrier densities $n_i(t, z)$, $i = 1$ to 4 (i : subband index) is evaluated as a function of time and a waveguide position according to Suzuki's approach [18]. In the second part, a propagation of CW probe light that is coupled with interband polarization [14] is simulated by the FDTD method, where $n_i(t, z)$ obtained at the first part of the calculation is used to evaluate the interband polarization. The pump pulse is injected either the left edge (forward pump case) or the right edge (backward pump case) of the waveguide, while the CW probe light is always injected from the left side. The phase change ($\Delta\phi(t)$) in the probe is evaluated at the right edge of the waveguide, where the probe electric field is fitted by $E(t) = E_0 \cos(\omega t + \Delta\phi(t) + \phi_0)$. Here, ω and ϕ_0 are the optical frequency of CW probe light and phase offset, respectively. The time in horizontal axis of Fig. 4(b) is defined such that a pump intensity peak arrives at the input position, i.e., the left edge for forward pump, and the right edge for backward pump, at 4 ps.

As shown in Fig. 4(a), the peak intensity in the pump

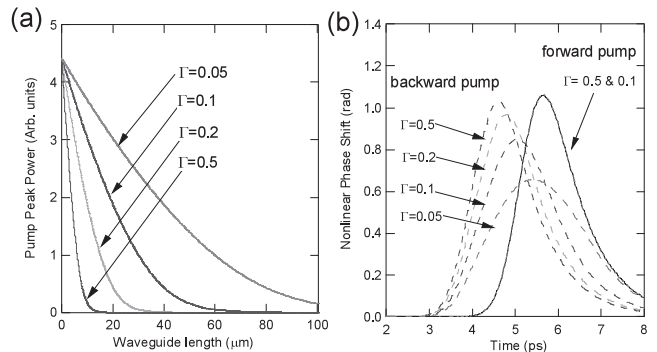


Fig. 4 (a) Pump peak intensity profile along the waveguide (b) nonlinear phase shift occurred on cw probe light as a function of time.

pulse attenuates as it propagates along the waveguide, where absorption magnitude of the waveguide is varied by adjusting a waveguide confinement factor (Γ). Note that the roll of the optical confinement factor in the simulation is only for adjusting a waveguide absorption coefficient, thereby examining the effect of a pump penetration depth on the XPM magnitude qualitatively. So the optical confinement factor used here does not reflect a value in the actual waveguide. Figure 4(b) shows a temporal phase shift imposed on the CW probe monitored at right edge of the waveguide. In the case of forward pump, the temporal phase change is not affected by a magnitude of waveguide absorption coefficient. In contrast, the temporal phase change becomes weak and broadened in the case of backward pump, as the absorption coefficient is reduced, meaning that a pump pulse penetrates more deeply into the waveguide. But in the case of strong attenuation of pump such as $\Gamma = 0.5$, an amount of phase shift in the backward propagation is almost same as that in forward one. This corresponds to the situation in the actual experiment where the pump penetration depth is much smaller than the spatial extension of the pump pulse in the waveguide.

3. All-Optical Demultiplexing

The experimental setup for all optical demultiplexing from 160- to 40 Gb/s by a MZI-ISBT switch is shown in Fig. 5. Two actively mode-locked fiber lasers (MLFLs) with a pulse width of 1.7 ps and repetition rate of 10 GHz are used as the control ($\lambda_c = 1560$ nm) and signal ($\lambda_s = 1541$ nm) light sources. The 10-GHz optical clock pulse from MLFL1 is data-coded at 10 Gb/s with a pseudo-random bit sequence (PRBS = $2^7 - 1$) using a LiNbO₃ intensity modulator. Then, the 10-Gb/s signal is multiplexed to generate 40-Gb/s signal using a fiber-based multiplexer that maintains the PRBS sequence. The 40-Gb/s signal is further multiplexed to generate 160-Gb/s OTDM signal pulse (40-Gb/s \times 4 channels) by another multiplexer. The 40-Gb/s signal before the second multiplexer is used for a bit error rate (BER) measurement in the case of a back-to-back. The 10-GHz pulse from MLFL2 is multiplexed to attain a 40-GHz control light that is split into two fiber lines for bi-directional pumping. The control

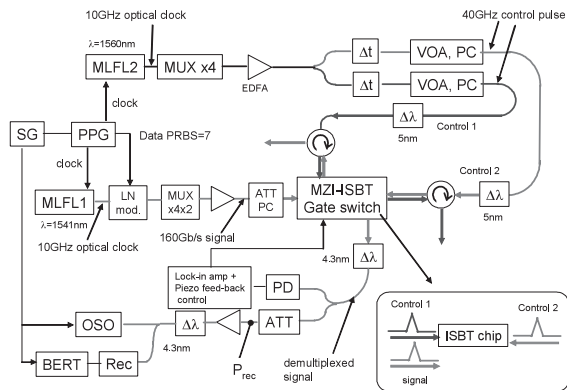


Fig. 5 Experimental setup for all-optical demultiplexing.

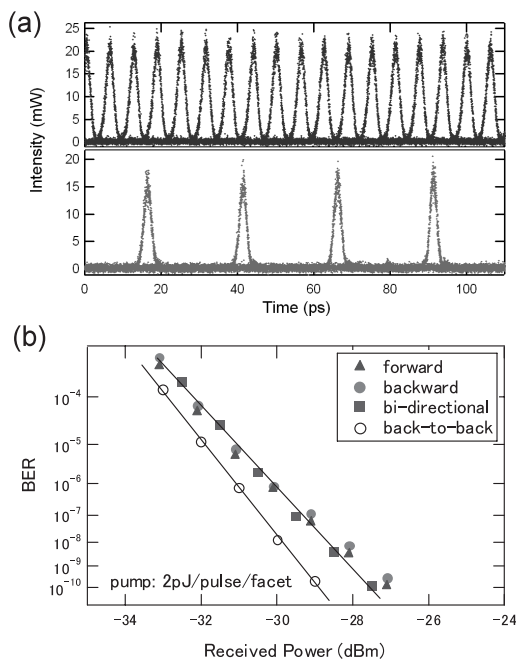


Fig. 6 (a) Eye diagram of demultiplexed 40-Gb/s signal with bi-directional pump. (b) Result of BER measurement with pump configurations of bi-directional and forward and backward pump.

and the OTDM signal pulses are injected into the MZI-ISBT switch module via the pump-in and probe-in ports, respectively. The intense control pulse opens a gate of the switch module at 40 GHz to extract a specific 40-Gb/s channel from the OTDM input signals by adjusting two optical-delay lines at the outside of the module. The 40-Gb/s demultiplexed signal after a receiver is further demultiplexed to 4×10 -Gb/s sub-channels by an electrical demultiplexer to evaluate BERs by an error rate detector. The received power is defined as a power injected into a pre-amplifier just before the receiver.

Figure 6(a) shows eye diagrams of the 160-Gb/s input OTDM signal (upper) and the demultiplexed 40-Gb/s signal (lower) measured by an optical sampling scope with 500-GHz band width. For the demultiplexing experiment, control pulse energy of 2 pJ/pulse/facet (total 4 pJ) is input

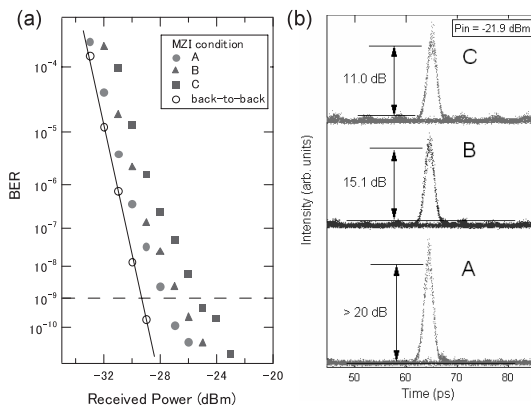


Fig. 7 (a) BER measurement results for different MZI interference condition and (b) corresponding eye diagram of demultiplexed 40-Gb/s signal.

into the MZI-ISBT module by the bi-directional pump configuration as mentioned before. While the average optical power injecting into the waveguide per facet is 80 mW that was kept below the damage threshold of ~ 100 mW, phase shift is doubled due to the bi-directional pump configuration. As shown in Fig. 6(a), the demultiplexed 40-Gb/s signal has an open and clear eye that is fairly identical to the eye diagram of 160-Gb/s input signal, indicating an excellent performance of demultiplexing. To investigate quantitatively the demultiplexing performance of the MZI-ISBT switch, we measured BER of the 40-Gb/s demultiplexed signal. Figure 7 shows the result of the BER measurement for the demultiplexed 40-Gb/s data pulses as a function of the optical power received by the pre-amplifier. The control pulse ($2 \text{ pJ/pulse} \times 2$) is injected in the bi-directional pump configuration. The power penalty measured from the back-to-back line is as low as 1.3 dB at a BER of 10^{-9} .

We also measured BER for three different pump configurations, i.e., bi-directional pump and single pump (co- or counter propagations) in Fig. 6(b). We found that BER curves for three pump configurations are almost identical in the BER range larger than $\sim 10^{-6}$, so a power penalty has almost identical with each other in the corresponding BER range. On the other hand, a slight decrease in the power penalty is observed for the bi-directional pump case in the BER range less than $\sim 10^{-6}$, i.e., 1.3 dB for bi-directional pump, 1.6 dB for forward pump, and 1.9 dB for backward pump at BER of 10^{-9} . This slight improvement of the power penalty by 0.3–0.6 dB for bi-directional pump case is attributed to the increase of nonlinear phase shift twice compared with single pump case. As discussed previously, the pump propagation direction with respect to the signal propagation in the waveguide does not affect an amount of phase shift due to short penetration depth of the pump ($\sim 30 \mu\text{m}$). Thus, the forward pump configuration attains almost same amount of phase shift as the backward case, and a bi-directional pump setup merely increases the phase shift two times, compared with a single pump case.

As discussed above, the BER curves for three configurations are almost identical except for the slight improve-

ment of the power penalty in the BER range less than $\sim 10^{-6}$. This result indicates that a nonlinear phase shift of only ~ 0.2 rad induced by 2 pJ-pump pulse injected from one facet is enough large to achieve the demultiplexed signal with high Q factor corresponding to error free condition. Signal attenuation at the “on” state caused by a phase shift of 0.2 rad is still as low as -20 dB, measured from the reference point of the most constructive interference condition, while that of “off” state has much lower value of -47 dB due to a superior performance of this interferometer module. Thus a switching extinction ratio is as high as 27 dB even for input pulse energy of only 2 pJ. To attain a high signal attenuation at the “off” state, a power balance of the asymmetric MZI is adjusted by a half wave plate before the first polarization beam splitter shown in Fig. 1(b), while a phase bias is adjusted by a mirror mounted on a piezo actuator, and actively stabilized by a feedback loop.

In contrast, we found that the power penalty is mainly affected by signal attenuation at the “off” state, i.e., the power penalty increases rapidly as the attenuation at the “off” state becomes worse. Figures 7(a) and (b) show BER curves and corresponding demultiplexed 40-Gb/s signal eye patterns, respectively, measured with different signal attenuation at the “off” state. The attenuation at the “off” state is intentionally deteriorated by unbalancing a signal splitting ratio between two MZI arms. As seen in eye patterns in Fig. 7(b), unbalanced MZI conditions of “B” and “C” can be assured by an appearance of a residual 160-Gb/s signal

that is not demultiplexed. In this experiment, the control pulse with 2 pJ/facet is injected into the module with the bi-directional pump configuration. The power penalty increases from 1.5 dB to 4.1 dB at BER of 10^{-9} , while it increases from 0.5 dB to 2 dB at BER of 10^{-4} . Note that the on/off switching extinction ratio value denoted in Fig. 7(b) was evaluated directly by a eye pattern waveform, hence the value of on/off extinction ratio of 20 dB in MZI condition “A” was under estimated due to a dark noise of optical sampling scope. It should be larger than 20 dB.

In the above 40-Gb/s demultiplexing experiment, a injection timings of forward and reverse control pulse are adjusted to extract a specific 40-Gb/s signal channel from multiplexed from 40-Gb/s \times 4 channels. Similarly, an injection timing of two control pulses can be adjusted to perform a demultiplexing at higher bit rate of 80 Gb/s. Figure 8(a) and (b) shows the result of the 80-Gb/s demultiplexing, where 160-Gb/s input signal can be regarded as multiplexed from 80-Gb/s \times 2 channels. Although signal amplitude in the demultiplexed 80-Gb/s signal is weaker than the case of 40-Gb/s demultiplexing, a clear and open eye can be seen. The result here illustrates the effectiveness of the bi-directional pump scheme to increase a bit rate of demultiplexing without damage in a waveguide facet due to a high optical power injection.

4. Conclusion

We have discussed XPM efficiency in a InGaAs/AlAsSb CDQW waveguide and the BER performance of all-optical demultiplexing operation for three pump configurations, i.e., forward-, backward-, and bi-directional cases. We found that XPM efficiency does not depend on injection direction of pump, since a region of the waveguide where a nonlinear phase shift appears is limited to a few tens μm from the input facet due to a strong attenuation of the pump intensity along a propagation direction. BER measurements on 40-Gb/s demultiplexed signal show that BER curves for three pump configurations are almost identical in the BER range larger than $\sim 10^{-6}$, so a power penalty is almost same for all cases in the corresponding BER range. On the other hand, a slight decrease in the power penalty is observed for the bi-directional pump case in the BER range less than $\sim 10^{-6}$, i.e., the penalty is 1.3 dB at BER of 10^{-9} for the bi-directional pump case, while it increases by 0.3–0.6 dB for single pump cases. A power penalty is influenced mainly by signal attenuation at “off” state due to the insufficient nonlinear phase shift, achievable value of which is suppressed by the current low XPM efficiency of ~ 0.1 rad/pJ and the damage threshold power of 100 mW in a waveguide facet.

Acknowledgments

The work is partly supported by the New Energy and Industrial Technology Development Organization (NEDO).

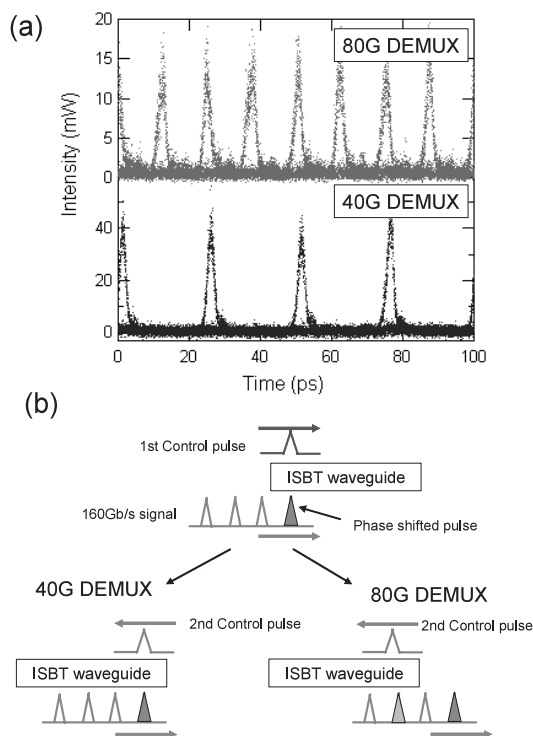


Fig. 8 (a) Eye diagram of 80-Gb/s (upper) and 40-Gb/s demultiplexed signal by bi-directional pump configurations. (b) Schematic of injection timing of control pulses for 40-Gb/s and 80-Gb/s demultiplexing.

References

- [1] K.J. Blow, N.J. Doran, and B.P. Nelson, "Demonstration of the nonlinear fibre loop mirror as an ultrafast all-optical demultiplexer," *Electron. Lett.*, vol.26, pp.962–963, 1990.
- [2] M. Nakazawa, E. Yoshida, T. Yamamoto, E. Yamada, and A. Sahara, "TDM single channel 640 Gbit/s transmission experiment over 60 km using 400 fs pulse train and walk-off free, dispersion flattened nonlinear optical loop mirror," *Electron. Lett.*, vol.34, pp.907–908, 1998.
- [3] K.E. Stubkjaer, "Semiconductor optical amplifier-based all-optical gates for high-speed optical processing," *IEEE J. Sel. Top. Quantum Electron.*, vol.6, pp.1428–1435, 2000.
- [4] Y. Ueno, S. Nakamura, and K. Tajima, "Nonlinear phase shifts induced by semiconductor optical amplifiers with control pulses at repetition frequencies in the 40–160-GHz range for use in ultrahigh-speed all-optical signal processing," *J. Opt. Soc. Am. B*, vol.19, pp.2573–2589, 2002.
- [5] E. Tangdiongga, Y. Liu, H. de Waardt, G.D. Khoe, A.M. J. Koonen, H.J.S. Dorren, X. Shu, and I. Bennion, "All-optical demultiplexing of 640 to 40 Gbits/s using filtered chirp of a semiconductor optical amplifier," *Opt. Lett.*, vol.32, pp.835–837, 2007.
- [6] T. Akiyama, N. Georgiev, T. Mozume, H. Yoshida, A.V. Gopal, and O. Wada, "1.55- μm picosecond all-optical switching by using intersubband absorption in InGaAs-AlAs-AlAsSb coupled quantum wells," *IEEE Photonics Technol. Lett.*, vol.14, pp.495–497, 2002.
- [7] T. Simoyama, S. Sekiguchi, H. Yoshida, J. Kasai, T. Mozume, and H. Ishikawa, "Absorption dynamics in all-optical switch based on intersubband transition in InGaAs-AlAs-AlAsSb coupled quantum wells," *IEEE Photonics Technol. Lett.*, vol.19, pp.604–606, 2007.
- [8] N. Iizuka, K. Kaneko, and N. Suzuki, "Sub-picosecond all-optical gate utilizing an intersubband transition," *Opt. Express*, vol.13, pp.3835–3840, 2005.
- [9] Y. Li, A. Bhattacharyya, C. Thomidis, T.D. Moustakas, and R. Paiella, "Nonlinear optical waveguides based on near-infrared intersubband transitions in GaN/AlN quantum wells," *Opt. Express.*, vol.15, pp.5860–5865, 2007.
- [10] R. Akimoto, B.S. Li, K. Akita, and T. Hasama, "Subpicosecond saturation of intersubband absorption in (CdS/ZnSe)/BeTe quantum-well waveguides at telecommunication wavelength," *Appl. Phys. Lett.*, vol.87, p.181104, 2005.
- [11] G.W. Cong, R. Akimoto, K. Akita, T. Hasama, and H. Ishikawa, "Low-saturation-energy-driven ultrafast all-optical switching operation in (CdS/ZnSe)/BeTe intersubband transition," *Opt. Express*, vol.15, pp.12123–12130, 2007.
- [12] H. Tsuchida, T. Shimoyama, H. Ishikawa, T. Mozume, and M. Nagase, "Cross-phase-modulation-based wavelength conversion using intersubband transition in InGaAs/AlAs/AlAsSb coupled quantum wells," *Opt. Lett.*, vol.32, pp.751–753, 2007.
- [13] H. Ishikawa, H. Tsuchida, K.S. Abedin, T. Shimoyama, T. Mozume, M. Nagase, R. Akimoto, T. Miyazaki, and T. Hasama, "Ultrafast all-optical refractive index modulation in intersubband transition switch using InGaAs/AlAs/AlAsSb quantum wells," *Jpn. J. Appl. Phys.*, vol.46, pp.L157–L160, 2007.
- [14] G.W. Cong, R. Akimoto, M. Nagase, T. Mozume, T. Hasama, and H. Ishikawa, "Mechanism of ultrafast modulation of refractive index of photoexcited InGaAs/AlAsSb quantum well waveguides," *Phys. Rev. B*, vol.78, p.075308, 2008.
- [15] R. Akimoto, T. Simoyama, H. Tsuchida, S. Namiki, C.G. Lim, M. Nagase, T. Mozume, T. Hasama, and H. Ishikawa, "All-optical demultiplexing of 160–10 Gbit/s signals with Mach-Zehnder interferometric switch utilizing intersubband transition in InGaAs/AlAs/AlAsSb quantum well," *Appl. Phys. Lett.*, vol.91, p.221115, 2007.
- [16] K.S. Abedin, G.W. Lu, T. Miyazaki, R. Akimoto, and H. Ishikawa, "High-speed all-optical modulation using an InGaAs/AlAsSb quantum well waveguide," *Opt. Express.*, vol.16, pp.9684–9690, 2008.
- [17] M. Nagase, R. Akimoto, T. Simoyama, G.W. Cong, T. Mozume, T. Hasama, and H. Ishikawa, "Enhancement of XPM efficiency in InGaAs/AlAsSb coupled quantum wells using InAlAs coupling barriers," *IEEE Photonics Technol. Lett.*, vol.20, pp.2183–2185, 2008.
- [18] N. Suzuki, N. Iizuka, and K. Kaneko, "Simulation of ultrafast GaN/AlN intersubband optical switches," *IEICE Trans. Electron.*, vol.E88-C, no.3, pp.342–348, March 2005.



Ryoichi Akimoto received the B.S., M.S. and Ph.D. degrees in Department of Material Physics, Faculty of Engineering Science from Osaka University in 1989, 1991 and 1994, respectively. In 1994, he joined Electrotechnical Laboratory, Ministry of International Trade and Industry. Since 2001, he was with Photonics Research Institute, National Institute of Advanced Industrial Science and Technology (AIST). Since 2005, he has been with Ultrafast Photonic Devices Laboratory, AIST. He has engaged in research on ultrafast phenomena in semiconductor quantum structures and its applications to ultrafast opto-electronic devices in the framework of Femtosecond Technology Project (1995–2004). He is currently involved in the development of ultrafast all-optical switching devices based on intersubband transition in III-V and II-VI-based semiconductor quantum wells. He is a member of Japan Society of Applied Physics and the Physical Society of Japan.



Guangwei Cong received the B.E., M.E. and Ph.D. degrees respectively from Hunan University in 2000, Beijing University of Science and Technology in 2003, and Institute of Semiconductors, Chinese Academy of Sciences in 2006. In 2006, he joined the Ultrafast Photonics Devices Laboratory, National Institute of Advanced Industrial Science and Technology (AIST) at Tsukuba as a postdoc. Since 2007, he becomes a JSPS fellow supported by the Japan Society for the Promotion of Science. Currently,

his research focuses on the devices and related physics of ultrafast all-optical switching devices based on intersubband transition. He is a member of Japan Society of Applied Physics.



Masanori Nagase was born in Ibaraki, Japan, in 1973. He received the B.Eng. degree from the University of Tsukuba, Japan, in 1996. He received the M.Eng. and Dr.Eng. degrees from Tokyo Institute of Technology, Japan, in 1998 and 2001 respectively. He joined the National Institute of Advanced Industrial Science and Technology (AIST) in 2004. Since then, he has been engaged in development of all-optical switch utilizing the intersubband transition in III-V based semiconductor quantum wells. He is a member of Japan Society of Applied Physics.



Teruo Mozume received M.S. degree in Physical Chemistry from Osaka University, Osaka Japan, and Ph.D. degree in electrical engineering from The Tokyo Institute of Technology, Tokyo, Japan. From 1990 to 1996, he was with Hitachi Central Research Laboratory, Tokyo, Japan, where he was engaged in the research and development of InP based hetero-bipolar transistors for the 40 Gbps optical communication networks. From 1996 to 2004, he was with The Femtosecond Technology Research Association, Tsukuba, Japan, where he was involved in the research and development of the ultrafast all-optical switches using the intersubband transitions in III-V QWs. In 2004, he moved to National Institute of Advanced Industrial Science and Technology (AIST) and has continued the research and development of the ultrafast all-optical switches. His areas of research interest are MBE growth and characterization of III-V materials and development of III-V optical and electrical devices. Dr. Mozume is a member of the IEEE Laser and Electro-Optical Society, IEEE Electron Device Society, The Japan Society of Applied Physics, and The Physical Society of Japan.

research Association, Tsukuba, Japan, where he was involved in the research and development of the ultrafast all-optical switches using the intersubband transitions in III-V QWs. In 2004, he moved to National Institute of Advanced Industrial Science and Technology (AIST) and has continued the research and development of the ultrafast all-optical switches. His areas of research interest are MBE growth and characterization of III-V materials and development of III-V optical and electrical devices. Dr. Mozume is a member of the IEEE Laser and Electro-Optical Society, IEEE Electron Device Society, The Japan Society of Applied Physics, and The Physical Society of Japan.



Hiroshi Ishikawa received B.S. degree in 1970 and M.S. degree in 1972 both from Tokyo Institute of Technology. He joined Fujitsu Laboratories Ltd. in 1972. He received Doctor of Eng. degree from Tokyo Institute of Technology in 1984. In Fujitsu Labs., he engaged in the research and development of optical semiconductor devices. He invented and developed a Fabry-Perot laser named VSB laser used in TPC-3 undersea cable systems and many trunk lines. He developed DFB lasers including modulator integrated lasers for high bit-rate systems and tunable narrow line-width lasers for coherent systems. He proposed the use of InGaAs substrate for temperature robust $1.3\ \mu\text{m}$ lasers, and demonstrated high T_0 . He also worked for quantum dot lasers and nonlinear optical devices. Since 2001, he engaged in the research and development of ultrafast optical switches at The Femtosecond Technology Research Association. In 2004, he moved to National Institute of Advanced Industrial Science and Technology, and he is director of Ultrafast Photonic Devices Laboratory. He is a member of Japan Society of Applied Physics, The Physical Society of Japan, and IEEE (Fellow).

He developed DFB lasers including modulator integrated lasers for high bit-rate systems and tunable narrow line-width lasers for coherent systems. He proposed the use of InGaAs substrate for temperature robust $1.3\ \mu\text{m}$ lasers, and demonstrated high T_0 . He also worked for quantum dot lasers and nonlinear optical devices. Since 2001, he engaged in the research and development of ultrafast optical switches at The Femtosecond Technology Research Association. In 2004, he moved to National Institute of Advanced Industrial Science and Technology, and he is director of Ultrafast Photonic Devices Laboratory. He is a member of Japan Society of Applied Physics, The Physical Society of Japan, and IEEE (Fellow).



Hidemi Tsuchida received the B.E., M.E. and Dr.Eng. Degrees in electronics engineering from the Tokyo Institute of Technology in 1979, 1981 and 1984, respectively. In 1984, he joined the Electrotechnical Laboratory, the Ministry of International Trade and Industry. From 1991 to 1992, he was a visiting researcher at the California Institute of Technology. Since 2001 he has been with the National Institute of Advanced Industrial Science and Technology (AIST), where he is currently a Prime Senior Researcher of the

Photonics Research Institute. His research interests are in optical signal processing for high-capacity photonic network and quantum communication. He received Niwa Memorial Award in 1984. He is a member of the Japan Society of Applied Physics, Optical Society of Japan, Optical Society of America, and Institute of Electrical and Electronics Engineers.



Toshifumi Hasama received the B.S., M.S. and Ph.D. degrees in engineering from Kyoto University in 1976, 1978 and 1981, respectively. In 1981, he joined Electrotechnical Laboratory, Ministry of International Trade and Industry. Since 2001, he was with Photonics Research Institute, National Institute of Advanced Industrial Science and Technology (AIST). Since 2005, he has been with Ultrafast Photonic Devices Laboratory, AIST. He has engaged in research on ultrafast quantum electronics and ultrafast opto-

electronics since 1989. He is a member of Japan Society of Applied Physics and the Laser Society of Japan.